FULL ENVELOPE ROBUST CONTROL LAW FOR THE BELL-205 HELICOPTER

Alex J. Smerlas*, Ian Postlethwaite and Daniel J. Walker
Control Systems Research
Department of Engineering
University of Leicester
Leicester LE1 7RH
U.K.

*** 1996 European Rotorcraft Forum ***
16-19 September, 1996, Brighton, UK

Abstract

In this paper, a set of controllers is designed for the Bell-205 airborne simulator [2]. Each controller provides robust stability against coprime factor uncertainty and forces the system to follow a pre-specified reference model [6]. A global control law is synthesised by interpolating the compensator gains by using three different scheduling laws. Comparisons are performed in terms of achievable phase and gain margins so the designer can trade-off performance and robustness over the whole envelope. The Aeronautical Design Dtandard (ADS-33C) is used to test the control laws at the various operating points.

1 Introduction

The operational capabilities of combat and civil helicopters require advanced flight control systems with handling qualities tailored to the mission task. When required to operate at the limit of the vehicle's performance and in bad conditions, it is of primary importance to reduce the pilot's workload. Therefore the low level stabilisation and feedback control should be performed with respect to the following objectives:

i) Robust stability: the controller must stabilise the rotorcraft with respect to changes in non-linearities, turbulence and so on.

ii) Full envelope performance: the controller should allow the pilot to fly the helicopter with confidence in all operational modes.

Design methods such as H_∞ optimisation, can comply with the above requirements because they are inherently multivariable and guarantee a degree of robustness over and above an uncertainty model. Therefore, it may give better decoupling and can reduce the design effort significantly, when compared with the old one-loop-at-a-time methods. The H_∞ loop shaping approach used in this report is essentially a two stage design process. Firstly, the open-loop plant is cascaded with two compensators, to give a desired shape to the open loop frequency response. Secondly, closed loop design specifications are introduced, with a reference model, and the standard optimisation returns a stabilising controller.

The first step, the core of the design method, enables the designer to specify performance requirements by using the open loop nominal plant and simple loop shaping ideas. Compliance with robust stability requirements can be assessed quickly by inspecting the stability margin for the given singular value shape. All it takes is the solution of two riccati equations; no lengthy time simulations are necessary. Early approaches in H_∞ optimisation were dominated by mixed sensitivity approaches, which were vulnerable to pole-zero cancellations. In the loop shaping approach no pole-zero cancellation occurs in the closed loop system, except for a certain, special, class of plants [9]. Also, the uncertainty against which the plant is stabilised is broader than the multiplicative or additive perturbation models. The coprime factors are always stable, and no restriction is imposed on the number of right half-plane poles of the nominal and perturbed plants. When frequency loop shaping is not sufficient to satisfy the stringent specifications on the output response, a two-degrees-of-freedom control scheme is employed. The same loop shaping precompensators can be used, and the final controller can be found by a single γ-iteration.

In this work a 2DOF approach to the H_∞ loop-shaping design procedure, as introduced by Hoyle et.al. in [6], is applied to the Bell 205. The main objective is to design a full-authority control system that: a) robustly stabilizes the helicopter with respect to model uncertainty, b)provides high level of decoupling between the selected outputs and c) satisfies the ADS-33C level 1 criteria. In Walker et.al. [14] it was demonstrated on a high-bandwidth Lynx-type helicopter, that the 2DOF approach provides an elegant framework for designing control laws to meet strict performance requirements. Additionally, the advantage of these controllers is that they possess a particular structure [13] that can be used for practical implementation and scheduling across different operating point designs.

This paper is organised as follows: Section 2 contains some background material to the robust stabilisation problem and section 3 presents the controller structure. In section 4 we

[1]E-mail : ajs15@sun.engg.leicester.ac.uk.
[2]Operated by the Flight Research Laboratory, NRC, Canada

describe the controller designs as applied to the Bell 205 airborne simnulator. Finally , section 5 presents the results of the control law tests against the ADS-33C requirements.

2 Robust stabilisation

We will consider the stabilisation of a plant G which has a normalised left coprime factorisation

$$G = M^{-1}N. \qquad (1)$$

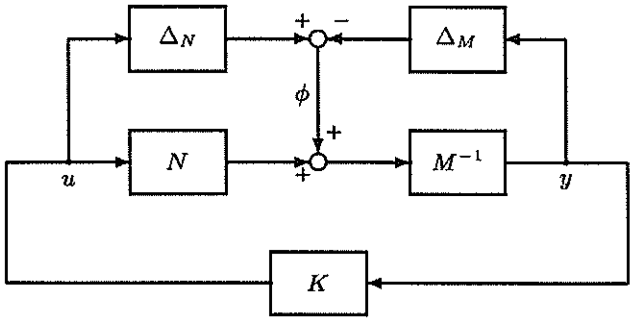

Figure 1: robust stabilisation problem

A perturbed plant model G_{pet} can then be written as

$$G_{pet} = (M + \Delta_M)^{-1}(N + \Delta_N) \qquad (2)$$

where Δ_M, Δ_N are stable unknown transfer functions which represent the uncertainty in the nominal plant model G. The objective of robust stabilisation is to stabilise the family of perturbed plants defined by

$$G_{pet} = \left\{(M + \Delta_M)^{-1}(N + \Delta_N) : \| \begin{bmatrix} \Delta_N & \Delta_M \end{bmatrix} \|_\infty < \epsilon\right\} \qquad (3)$$

where $\epsilon > 0$ is then the stability margin. The maximisation of this stability margin was introduced and solved by Glover and McFarlane [3].

For the perturbed feedback system of figure 1, the stability property is robust if and only if the nominal feedback system is stable and

$$\gamma \triangleq \left\| \begin{bmatrix} K \\ I \end{bmatrix} (I - GK)^{-1}M^{-1} \right\|_\infty \leq \frac{1}{\epsilon} \qquad (4)$$

The maximum stability margin ϵ are given by

$$\gamma_{\min} = \epsilon_{max}^{-1} = \left\{1 - \|[N \ \ M]\|_H^2\right\}^{-\frac{1}{2}} = (1 + \rho(XZ))^{\frac{1}{2}} \qquad (5)$$

where $\| \cdot \|_H$ denotes Hankel norm, ρ denotes the spectral radius, and for a minimal state-space realisation (A, B, C, D) of G, Z is the unique positive definite solution to the algebraic Riccati equation

$$A_z Z + Z A_z^T - ZC^T R^{-1} CZ + BS^{-1}B^T = 0 \qquad (6)$$

where

$$A_z = A - BS^{-1}D^T C$$
$$R = I + DD^T, \quad S = I + D^T D$$

and X is the unique positive definite solution of the following algebraic Riccati equation

$$A_z^T X + XA_z - XBS^{-1}B^T X + C^T R^{-1} C = 0 \qquad (7)$$

A controller which guarantees that

$$\left\| \begin{bmatrix} K \\ I \end{bmatrix} (I - GK)^{-1}M^{-1} \right\|_\infty \leq \gamma \qquad (8)$$

for a specified $\gamma > \gamma_{min}$, is given by

$$K \overset{s}{=} \left[\begin{array}{c|c} A_k & B_k \\ \hline C_k & D_k \end{array}\right] \qquad (9)$$
$$A_k = A + BF + \gamma^2(L^T)^{-1}ZC^T(C + DF) \qquad (10)$$
$$B_k = \gamma^2(L^T)^{-1}ZC^T \qquad (11)$$
$$C_k = B^T X \qquad (12)$$
$$D_k = -D^T \qquad (13)$$

where

$$F = -S^{-1}(D^T C + B^T X)$$
$$L = (1 - \gamma^2)I + XZ.$$

The procedure proposed by McFarlane and Glover in [8] has its systematic origin in [10] and has been applied to several industrial problems [11]

The two degrees-of-freedom approach, as introduced in [6] (Figure 2) includes a model matching problem in addition to the robust stability minimisation problem described above.

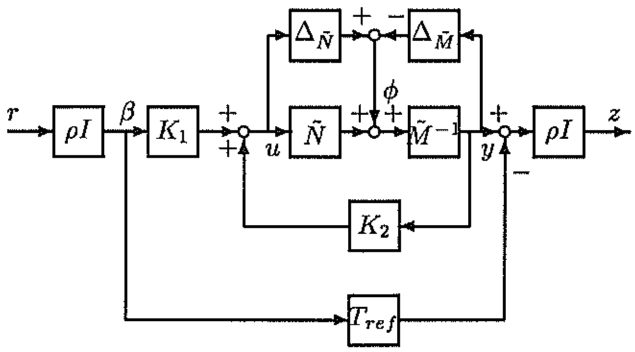

Figure 2: 2 DOF Scheme.

The closed loop response follows that of a specified model (T_{ref}) and the controller K is partitioned as K=$[K_1 \ K_2]$ where K_1 is the prefilter and K_2 is the feedback controller. The inner feedback controller K_2 is used to meet the robust stability requirements while the prefilter K_1 optimises the overall system to the command input. The use of the step response model is to ensure that

$$\gamma = \left\|(I - GK_2)^{-1}GK_1 - T_{ref}\right\| \infty \leq \gamma\rho^{-2} \qquad (14)$$

From figure 2 and the state space equations of the plant and the ideal model T_{ref} the problem can be formulated in the standard control configuration (SCC) form:

$$\begin{bmatrix} \dot{x} \\ \dot{x}_0 \\ \hline u \\ y \\ z \\ \hline \beta \\ y \end{bmatrix} = \left[\begin{array}{cc|cc|c} A & 0 & 0 & -H & B \\ 0 & A_0 & B_0 & 0 & 0 \\ \hline 0 & 0 & 0 & 0 & I \\ C & 0 & 0 & I & 0 \\ \rho F_s & -\rho^2 C_0 & 0 & \rho F_s & 0 \\ \hline 0 & 0 & \rho I & 0 & 0 \\ C & 0 & 0 & I & 0 \end{array}\right] \cdot \begin{bmatrix} x \\ x_0 \\ r \\ \phi \\ u \end{bmatrix}$$

3 Controller structure

Standard algorithms [1] performing the γ-iteration can be utilised to carry out the minimisation of the $\mathcal{H}_\infty$performance criterion. The controller was written in an observer form as depicted in figure 3 where the solution to the control Riccati equation X_∞ was partioned with respect to the generalised plant: $X_\infty = [X_{\infty 11}\ X_{\infty 12}]$:

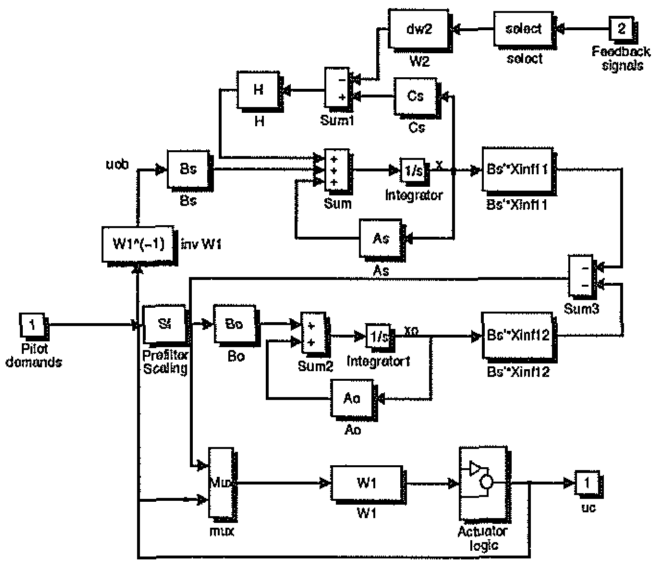

Figure 3: 2DOF controller structure

$$\begin{bmatrix} \dot{\hat{x}} \\ \dot{x}_0 \end{bmatrix} = \left[\begin{array}{c|c} A_c & B_c \\ \hline C_c & D_c \end{array}\right] \cdot \begin{bmatrix} \hat{x} \\ x_0 \end{bmatrix} + \left[\begin{array}{c|c} 0 & -H \\ \hline \rho B_0 & 0 \end{array}\right] \cdot \begin{bmatrix} r \\ y \end{bmatrix}$$

where

$$A_c = A + HC - BB^T X_{\infty 11}; \quad (15)$$

$$B_c = -BB^T X_{\infty 12}; \quad (16)$$

$$C_c = 0; \quad (17)$$

$$D_c = A_0; \quad (18)$$

.

$$u = -B^T [X_{\infty 11} X_{\infty 12}] \cdot \begin{bmatrix} \hat{x} \\ x_0 \end{bmatrix}$$

The prefilter K_1 (Figure 2) was also also scaled with a gain matrix $S_f = K_1^{-1}(0) \cdot K_2(0)$ so that the closed loop transfer function $(I - GK_2)^{-1} GK_1$ matched the unit matrix at the steady-state.

4 Controller design

The concept adopted for the controller design attempts to satisfy two basic requirements: Simplicity - it is essential that feedback and forward loops share the same structure throughout the flight envelope. Having a simple structure for the controller makes it easier to redesign a control law during the operational lifetime of a helicopter. Expandability - for a full envelope flight control law, it is desirable to have a range of responses. The controller architecture should be able to provide the pilot with a smooth transition between the flight modes (low/high speed flights) without degrading the achievable flying qualities.

The basic six degree-of-freedom model from [4] was used for the controller design. The model is using a quasi static rotor assumtion which does not incluse the dynamics of the tip-path plane. Therefore, the regressing flapping mode which has undamped natural frequency at 13.5 rad/sec is not modeled. Also, there is a considerable time delay between the control inputs and fuegelage responses; 0.093 sec in heave axis, 0.156 sec in pitch and roll and 0.187 sec in yaw axis [2]. This puts very strict limits on the achievable bandwidth. Some previous studies and consequences of the rotor dynamics effect on the Bell 205 responses can be found in [12].

The measurements slected for the feedback stabilisation loop are

- Vertical velocity (w)
- Pitch rate (q)
- Roll rate (p)
- Yaw rate (r)

There are two basic factors that brought us to arrive to this choice:

- The 4 measurements can be used over the entire envelope and hence the structure of the controller remains contant.
- The rates are measured in body axis and don't rely on earth based coordinate systems.

Linear designs have been carried out at two operating points namely 10 and 120 knots. The low speed design is used right down to hovering speeds and the 120 knot up to 130 knots. The same procedure is applied to both designs. The procedure in [10], [11] is followed:

i) Scale the inputs and outputs. All the inputs are in the same compatible units (cm) and therefore the input scaling is identity $I_{4 \times 4}$. The outputs are scaled such that 1 unit of coupling into outputs is equally undesirable. Vertical velocity (w) is scaled by 0.8 the pitch rate (q) by 0.2 and the roll and yaw rates by 0.2 and 0.2 respectively.

ii) First order Pade approximations were used to rerpesent the delays described above. For the design the delays were cascaded with the plant which resulted to a 10 state design model. No model reduction is performed.

iii) The singular values of the design plant were plotted against frequency. Next, each of the inputs is shaped using a dynamic precompensator in order to give the desired high gain in low frequency and low gain in high frequencies. Zeros are introduced to reduce the roll-off rate around the bandwidth to approximatelly $20dB$. The final form of the precompensator was

$$W_1 = \begin{bmatrix} \frac{s+5}{s} & 0 & 0 & 0 \\ 0 & \frac{s+10}{s} & 0 & 0 \\ 0 & 0 & \frac{s+10}{s} & 0 \\ 0 & 0 & 0 & \frac{s+5}{s} \end{bmatrix} \quad (19)$$

The postcompensator W_2 was set to identity since all the outputs are to be controlled.

iv) The final shaped plant was calculated as $G_s = GW_1$ and the singular values were aligned at 3 rad/sec. Note that alignment is the approximate inverse of the plant at 3 rad/sec. This essentially provides the cross-feeds to the loops necessary to decouple the outputs. The shaped plant ($G_s = GW_1K_a$) singular values are shown in figure 4.

v) Calculate the output injection riccati gain (H in the SCC) by solving the robust stabilisation problem for the shaped plant. The achievable spectral radius $\gamma = 2.3$ indicated good robustness and performance properties.

vi) Define a step response model (M_o), the model-matching parameter $\rho = I_4 * 1.4$ and build the standard control configuration. The ideal model incorporates first order transfer functions for heave and yaw axis and second order for pitch and roll.

vii) Minimise the cost (14) using the $\gamma - iteration$ and calculate the stabilising observer-based controller of figure 3. The forward and feedback controllers were easily obtained by partitioning the riccati solutions with respect to the SCC. Note the actuator logic and the W_1^{-1} blocks. The controller has been supplemented with a hanus anti-windup scheme which runs backwards the weight W_1 when actuator limiting occurs. Here, it is important to implement W_1 with approximate integrators as perturbations in the state-space can shift its poles to the right half complex plane.

viii) Plot the achieved loop shapes (figure 5) by cascading the $\mathcal{H}_\infty$controller with the shaped plant. Figure 6 shows the output sensitivity function plotted against frequency.

ix) The time responses are shown in figure 7. A step input of 5 m/sec, 0.5 rad/sec, 1 rad/sec and 1 rad/sec was applied to the collective, longitudinal and lateral cyclic and the pedals, respectively. The responses show good decoupling between the loops while all control surfaces (figure 8) remain within their physical limits .

A second controller at 120 knots was designed similarly to the low speed controller. The two controllers were interpolated linearly, as a square and as a cubic function of the forward speed respectively. At every operating point (where models were available) time and frequency responses were obtained. Figure 9 shows the spectral radius of the three different interpolating schemes and tables 1 and 2 show the achievable gain and phase margins for the linear and quadratic schedules.

5 Handling Qualities Assessment

Extensive handling qualities tests against ADS-33C confirmed that the control law remains robust and performes well over

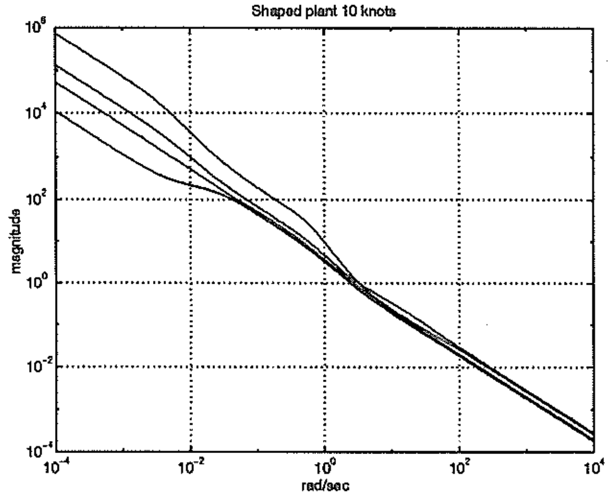

Figure 4: Shaped plant

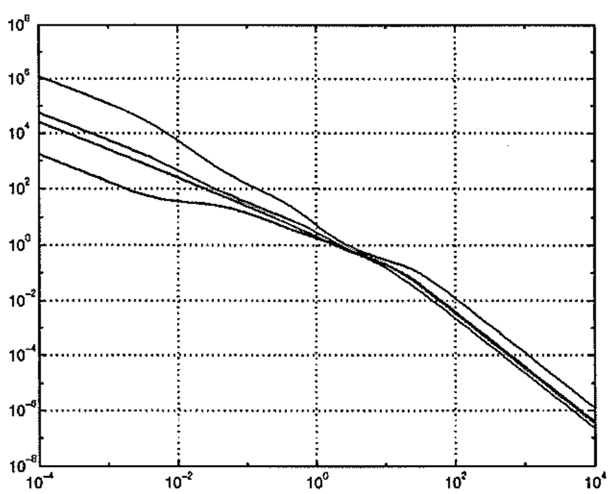

Figure 5: Achieved loop shapes

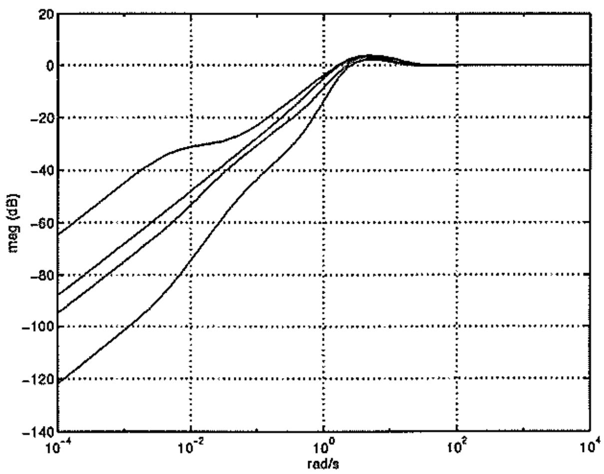

Figure 6: Output Sensitivity function

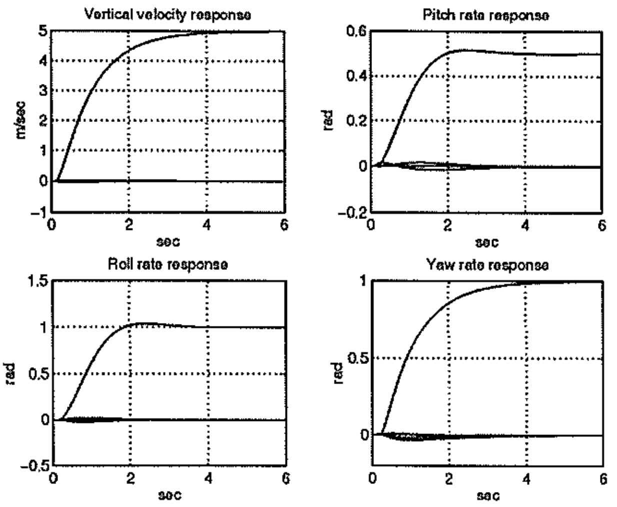

Figure 7: Time responses

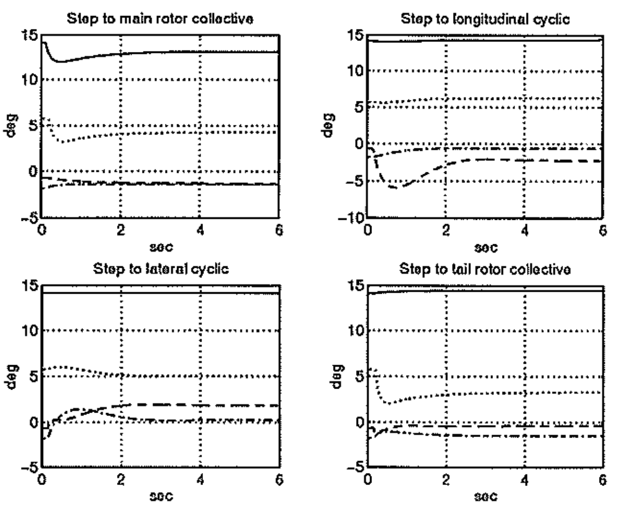

Figure 8: Control action. Coll.(-),long.cycl.(--),lat.cycl.(-.-),pedals(.)

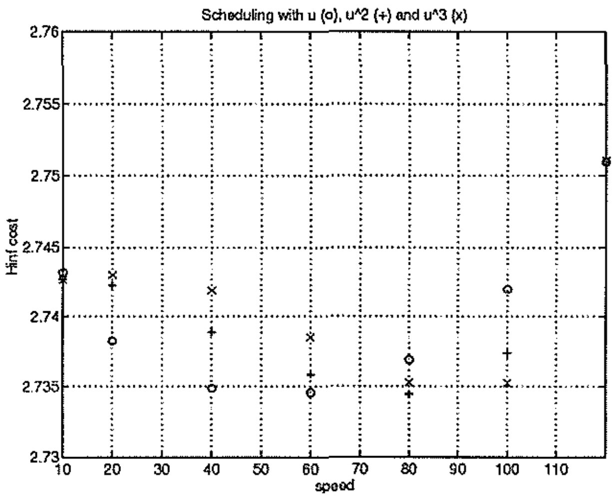

Figure 9: Cost function as a function of speed

Sensitivity peak	Gain magrin		Phase margin
1.5538	6.1048	0.5446	49.4291
1.6389	5.8155	0.5470	48.9156
2.0291	4.8001	0.5581	46.6361
2.4585	4.0566	0.5703	44.2641
2.5061	3.9899	0.5716	44.0096
2.1453	4.5693	0.5614	45.9804
1.5142	6.2509	0.5435	49.6707

Table 1: Gain/Phase margins, linear interpolation

Sensitivity peak	Gain magrin		Phase margin
1.5521	6.1112	0.5446	49.4398
1.8701	5.1625	0.5536	47.5501
2.7143	3.7261	0.5775	42.9149
3.5815	2.9595	0.6016	38.6651
3.8683	2.7824	0.6095	37.3618
3.2768	3.1821	0.5932	40.1039
1.5124	6.2575	0.5434	49.6813

Table 2: Gain/Phase margins, quadratic interpolation

the whole flight envelope. Tables 3, 4, 5, 6 show the short term frequency responses and the coupling for pitch and roll axes respectively.

Speed (knots)	Bandwidth (rad/sec)	Phase delay (sec)
10	2.82	0.06
20	2.72	0.05
40	2.63	0.05
60	2.58	0.05
80	2.57	0.05
100	2.59	0.05
120	2.68	0.05

Table 3: Pitch axis - Short term frequency response

6 Discussion

The analysis presented in this paper demonstrates the potential of advanced control techniques for real time applications. The observer-based controller in combination with anti-windup schemes provides good robust stability and performance over the whole flight envelope of the Bell 205 airborne simulator. The computations required to update the controller can be significantly reduced as the controller has a well-defined structure with only a few nonzero elements. Different scheduling approaches can be utilised to enhance the performance of the linear controllers. Further theoretical research is being conducted in this area.

Speed (knots)	Coupling (%)
10	2.90
20	3.68
40	4.76
60	4.18
80	4.00
100	3.27
120	2.68

Table 4: Pitch-to-roll coupling

Speed (knots)	Bandwidth (rad/sec)	Phase delay (sec)
10	2.87	0.07
20	2.86	0.07
40	2.87	0.07
60	2.87	0.07
80	2.85	0.07
100	2.87	0.08
120	2.83	0.08

Table 5: Roll axis - Short term frequency response

Speed (knots)	Coupling (%)
10	2.24
20	2.52
40	2.81
60	2.92
80	2.87
100	2.80
120	3.15

Table 6: Roll-to-pitch coupling

7 Acknowledgements

The authors would like to thank Mr. Stewart Baillie and Bill Gubbels of the Canadian Flight Research Laboratory for many helpful discussions regarding the Bell-205 helicopter model. We are also greatful to the UK Engineering and Physical Scienses Research Council for financial support.

References

[1] G.J. Balas, J.C. Doyle, K. Glover, A. Packard, and R. Smith. *μ-Analysis and Synthesis Toolbox: User's Guide*. MUSYN Inc. and The Mathworks, Inc., 1993.

[2] B.Gubbels. Private Communication. 1996.

[3] K. Glover and D. McFarlane. Robust Stabilization of Normalized Coprime Factor Plant Descriptions with $\mathcal{H}^\infty$-Bounded Ucertainty. *IEEE Transactions on Automatic Control*, 34(8):821–830, August 1989.

[4] R.K. Heffley, W.F. Jewell, J.M. Lehman, and R.A. Van Winkle. A Compilationand Analysis of Helicopter Handling Qualities Data. Contractor report 3144, NASA, 1979.

[5] J. Howitt. Matlab toolbox for handling qualities assessment of flight control laws. *IEE Control Conference*, pages 1251–1256, Scotland 1991.

[6] D. Hoyle, R. Hyde, and D.J.N. Limebeer. An $\mathcal{H}^\infty$ Approach to Two-Degree-Of-Freedom Design. *Proceedings of the IEEE CDC*, pages 1581–1585, December 1991.

[7] I.Postlethwaite, D.J.Walker, and A.Smerlas. Robust Control Law Design for the Bell-205 Helicopter. *Proceedings of the 21st rotorcraft forum,Saint-Petersburg,Russia*, vol. 3:No. VII.10.1–VII.10.7, Aug.30-Sept.1 1995.

[8] D. McFarlane and K. Glover. An $\mathcal{H}^\infty$ Design Procedure Using Robust Stabilization of Normalized Coprime Factors. *Proceedings of the 27th Conference on Decision and Control*, pages 1343–1348, December 1988.

[9] I.Postlethwaite M.C.Tsai and E.J.M.Geddes. Pole-zero cancellations and closed loop properties of an h_∞ mixed sensitivity design procedure. report 90-3, Department of Engineering, Leicester University, U.K., March 1990.

[10] R.A.Hyde. *The application of Robust Control to VSTOL Aircraft*. PhD thesis, Department of Engineering, Cambridge University,UK, 1991.

[11] S.Skogestad and I.Postlethwaite. *Multivariable Feedback Control*. John Wiley and Sons, 1996.

[12] J.M.Morgan S.W. Baillie and K.R.Goheen. Practical Experiences in Control Systems Design using the NCR Bell 205 Airborne Simulator. *Flight Mechanics Panel Symposium*, pages 27.1–27.12, January 1994.

[13] D.J. Walker. On the Structute of a 2-Degrees-Of-Freedom Fontroller. *International Journal of Control, vol. 63, No 6*, pages 1105–1127, 1996.

[14] D.J. Walker, I.Postlethwaite, J.Howitt, and N.P.Foster. Rotorcraft Flying Qualities Improvement Using Advanced Control. *American Helicopter Society/NASA Conference on Flying Qualities and Human Factors*, page No.2.3.1, 1993.